R.F. Note #122
NSCL
July 11, 2001

John Vincent

Accel K250 RF Resonator Optimization and Analysis

Introduction

A contract to build a 250 MeV proton cyclotron for medical application has recently been awarded to Accel [1]. The proposed cyclotron is based on a 1993 NSCL design.[2] The NSCL has agreed to assist Accel in achieving an optimized design for this machine. This paper is describes the design process and analysis for the radio frequency (rf) resonators of this machine.

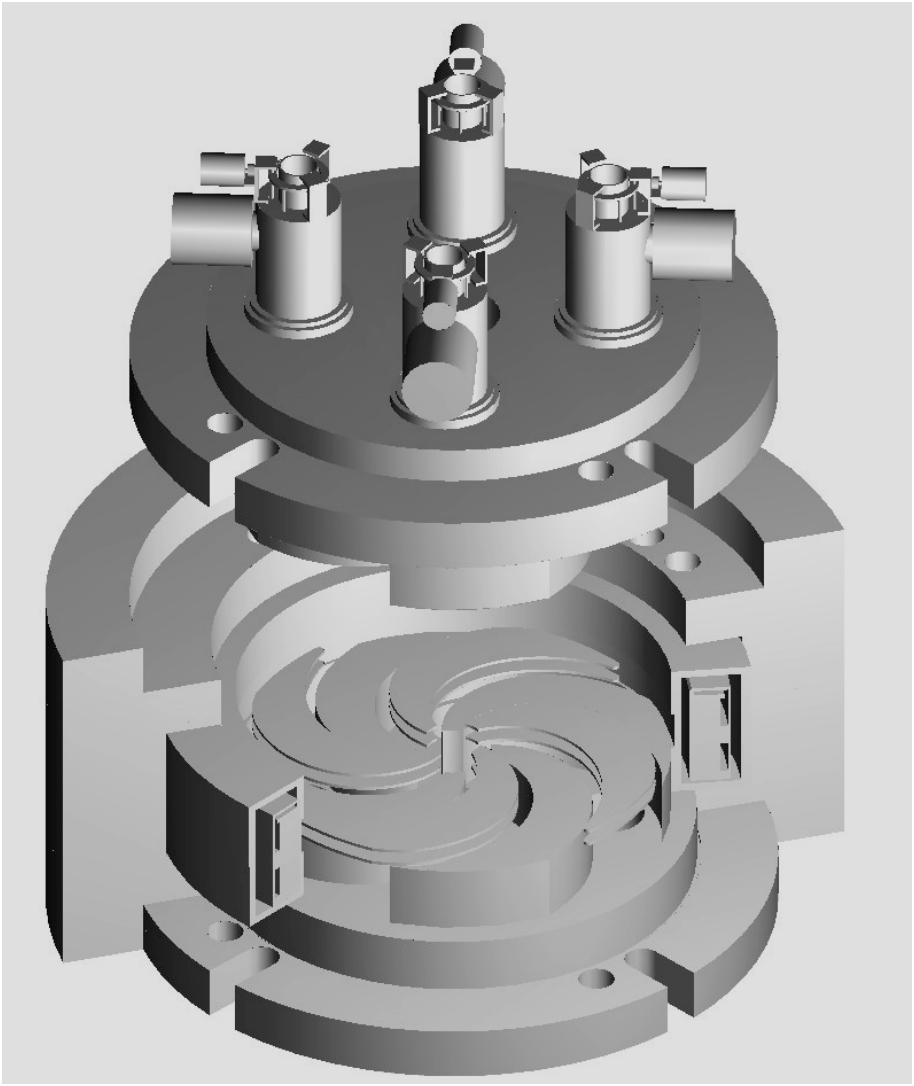

Figure 1: Cyclotron Illustration (rf tuning stems not shown)

Briefly, the cyclotron design consists of a four sector superconducting magnet sharing a common return yoke of 3098.8 mm outside diameter as illustrated in figure 1. The magnet design is almost entirely dominated by the requirements of the beam dynamics. The four spiral pole tips that protrude from each of the upper and lower magnet poles create the four sectors. The rf accelerating electrodes must fit within the space between the poles and thus assume the same basic spiral shape although they are still referred to as

"Dees" after the original classic cyclotron design. The dees may be thought of as the inner conductor of a transmission line mode resonator and the magnet pole and cryostat surfaces as the outer conductor. Tuning stems are connected at the appropriate point on the dees to 1) develop the required voltage profile along the dee, and 2) tune and maintain the proper resonant frequency. Each of the four rf resonators consists of two symmetric quarter wave sections joined at the cyclotron median plane. As a result, only one quarter wave section need be modeled and analyzed for purposes of electromagnetic optimization. The resultant circuit model of the quarter wave section will then be used as a repeated element in the overall circuit model to determine the various circuit modes of the system. In this system, two opposing resonators are conductively coupled together at the cyclotron center and the remaining two are capacitively coupled to them in the center. The desired circuit mode is the so-called pi-mode where the capacitively coupled resonators are operating 180 degrees apart in phase from the conductively coupled resonators.

Resonator Requirements

The requirements for the resonators include 1) a required gap spacing at the cyclotron center to aid injection and at the cyclotron outer radius to aid extraction, 2) a specified voltage ratio between the cyclotron center and outer radius, 3) a specified number of beam revolutions to obtain the full particle energy, 4) little or no sparking, and 5) minimal drive power. Based on experience, little or no sparking require that we try for < 60 KV/cm peak fields on reasonably smooth and rounded surfaces.

V_{inner}/V_{outer}	0.8
Center Gap	14 mm
Outer Gap	19 mm
Number of Turns	~ 500
Peak Electric Field	< 60 KV/cm

Table 1: The basic cyclotron rf parameters

Optimization Technique

The optimizations possible within the imposed system include 1) minimizing the power while keep the electric field below the sparking limit and 2) finding the proper location for the tuning stem to achieve the required voltage ratio. The second requirement will be found by trial and error placement using the computer circuit model after the resonator has been modeled. This section will derive a technique for minimizing the losses.

The optimization technique will use the knowledge that minimization of the dee capacitance while maintaining the needed accelerating voltage below the sparking limit

will minimize the power. This can be shown in various ways, a reasonably general way is too show that the conduction current in a resonator tends to be the integral of the displacement current. To show this, assume some simple quarterwave resonator that supports the following electric field in the space between the conductors.

$$\vec{E}_y = E_o \cos Kx \sin \omega t$$

The associated magnetic field is then:

$$\vec{H}_z = -\frac{1}{\mu}\int \vec{\nabla}\times \vec{E}\, dt = -\eta E_o \sin Kx \cos \omega t$$

$$\eta = \sqrt{\frac{\mu}{\varepsilon}}$$

In the space intervening the conductors the displacement current is:

$$\vec{\nabla}\times \vec{H}_z = \frac{d}{dx}\vec{H}_z = \frac{dD_y}{dt}$$

hence:

$$\vec{H}_z = \int_0^x \frac{dD_y}{dt} dx = \int_0^x J_D dx$$

At rf frequencies the conduction currents penetrate little into good conductors and may be calculated as surface currents “K” rather than volume currents “J”.

$$\vec{K}_x = \hat{n}\times \vec{H}_z = \int_0^x J_D dx \text{ : taken at the conductor surface.}$$

Since the losses in vacuum insulated cavities are predominantly conduction losses, the previous development makes clear that minimizing the displacement currents will reduce losses. Reduction of the displacement currents is accomplished by reducing the electric field at the conductor surface. This has the additional attribute of reducing sparking.

To optimize the resonator for acceleration, increasing the accelerating gaps and required voltage until either no decrease in losses is observed or until some imposed sparking threshold is exceeded reduces the power. The simple one-dimensional model used to derive the concept is illustrated in figure 2.

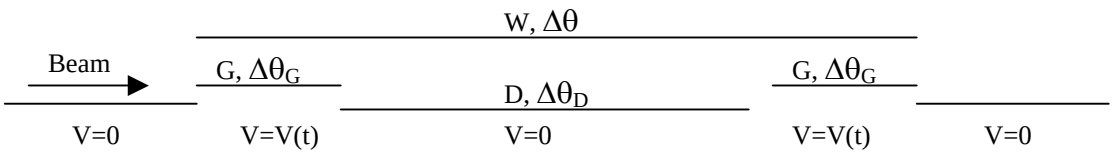

Figure 2: One Dimensional Accelerating Structure Illustration

The illustration in figure 2 shows the charged particle beam entering at the left from a region of 0 potential into the first accelerating gap then proceeding through a drift space of 0 potential then through another accelerating gap and finally into a region of zero potential again. In a conventional cyclotron, the regions of zero potential are between the spiral pole faces about the accelerating plane and the drift space is the region within the dee. The beam repeatedly traverses this space increasing the cyclotron radius as it increases energy. Since the beam traverses one revolution per rf cycle, the lengths of the spaces may also be specified by an angle. The mechanical angle and rf angle are approximately the same.

In this system, the displacement current and effective acceleration is increased as the gap is made smaller. However, this comes at a cost of increased conduction losses as shown in the previous development. If the gap is made larger the effective acceleration voltage is decreased and so is the conduction losses. To maintain a constant effective accelerating voltage the actual voltage must be increased as the gap is made bigger. The optimum gap decreases the conduction losses while maintaining an acceptable applied voltage level.

The equations governing the acceleration through this system are:

$$V_e = 2V_p \sin\left(\frac{\Delta\theta - \Delta\theta_G}{2}\right)\frac{\sin\Delta\theta_G}{\Delta\theta_G} \qquad (1)$$

where:

$$V(t) = V_p \sin(\omega t + \phi) \qquad (2)$$

As shown previously, since the magnitude of the conduction current is dependent on the displacement current, the losses may be represented by the following expression:

$$P_c \propto K\left(\int\left|\vec{D}\right|dx\right)^2 \approx Kl^2\left(\frac{V_p}{G}\right)^2$$

where “K” is some constant and “l” represents the guided path length.

If V_e is to be held constant then from expression (1) the above expression may be expressed as:

$$P_c = K\left[\frac{V_e}{\Delta\theta_G \sin\left(\frac{\Delta\theta - \Delta\theta_G}{2}\right)\frac{\sin(\Delta\theta_G)}{\Delta\theta_G}}\right]^2$$

To minimize Pc maximize:

$$f^* = \sin\left(\frac{\Delta\theta - \Delta\theta_G}{2}\right)\sin(\Delta\theta_G)$$

Figure 3 illustrates the effects predicted by this analysis:

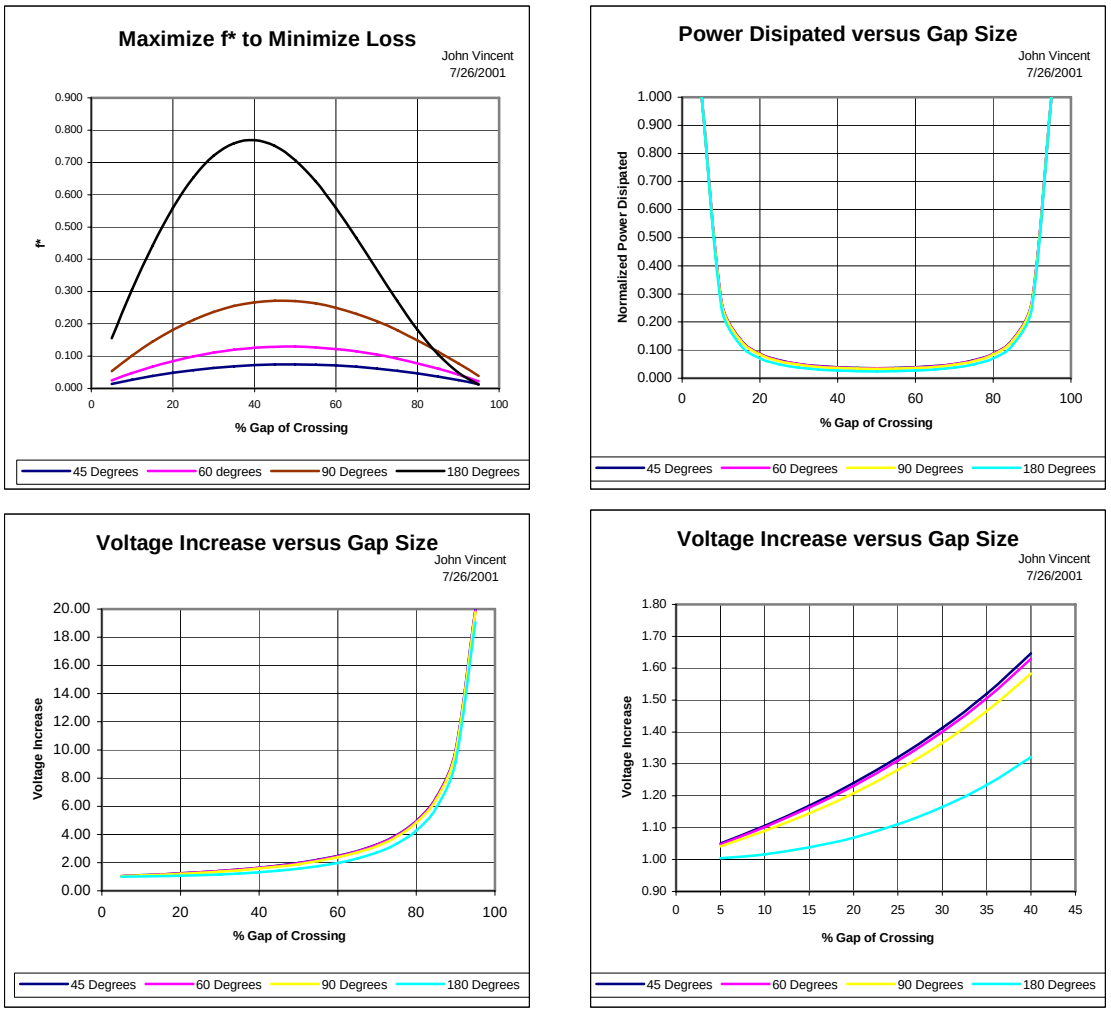

Figure 3: Optimization Law and its Effects

Design, Modeling, and Analysis

Figure 4 illustrates the application of the optimization technique. The power loss is dependent on the perpendicular distance from the dee-to-liner whereas the transit-time-factor is dependent on the angular path from dee-to-liner. A compromise was made to set the gap space to use 40% of the of the available transit time angle. This should still put the power required in the near minimum regime.

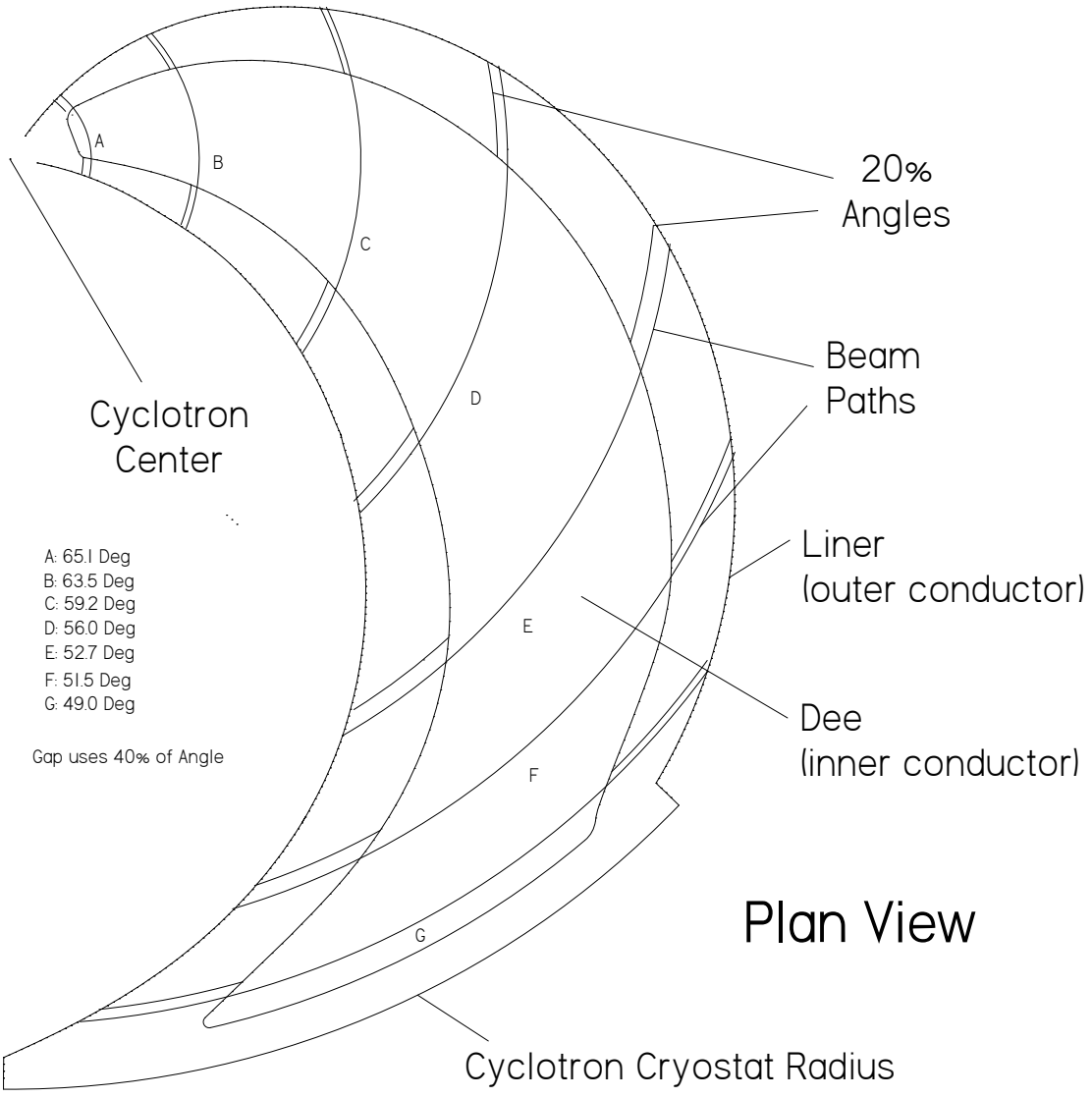

Figure 4: Development of the Dee Shape

Figure 5 illustrates the crossections selected that are used to determine a set of equivalent transmission lines describing the dee. Each cross-section is analyzed to determine the necessary parameters to equate power dissipated and characteristic impedance parameters of an equivalent infinitely long transmission line. Formulas developed elsewhere [3, 4] are applied to create equivalent lines for each segment.

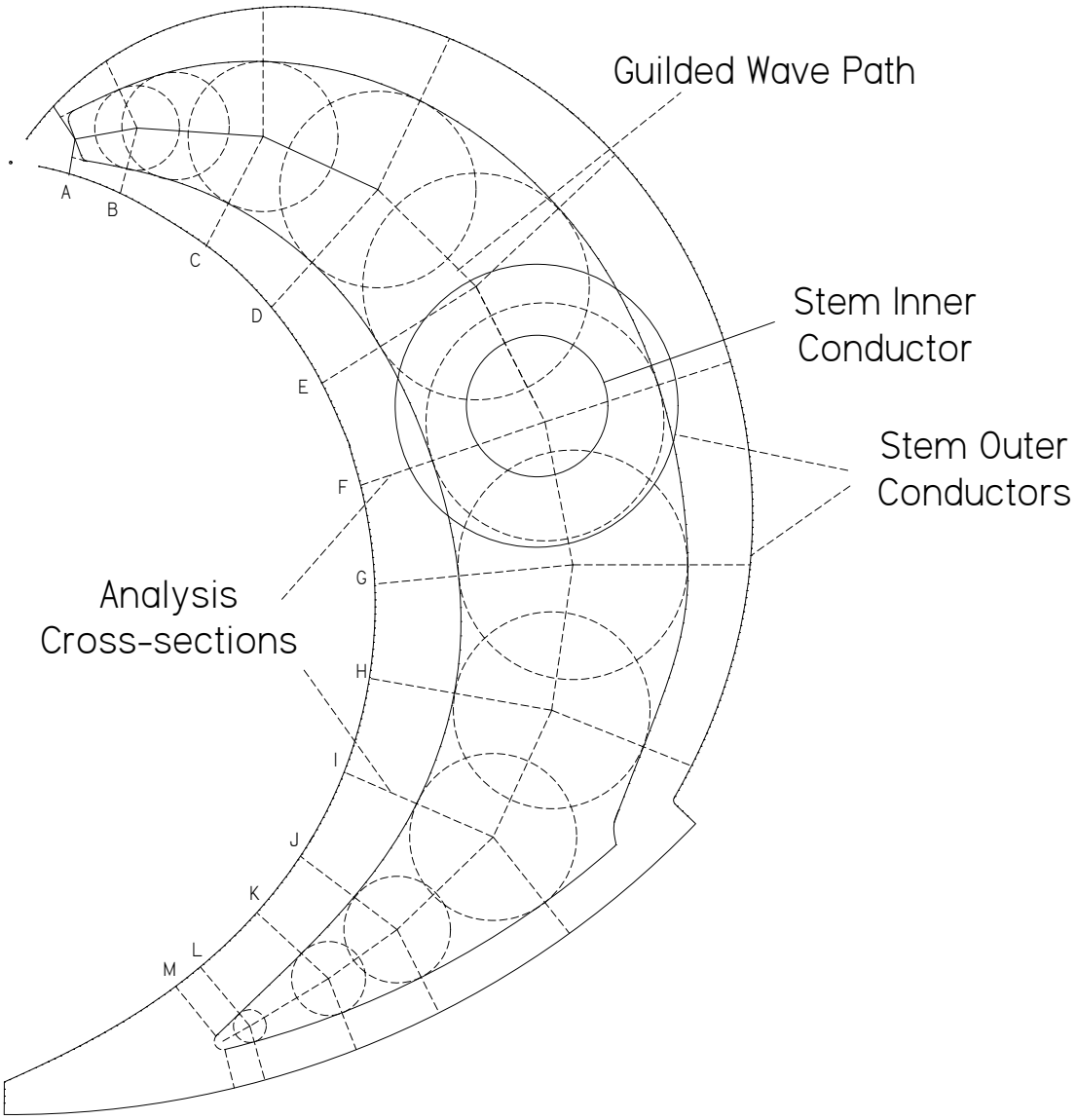

Figure 5: Cross-sections used to Develop the Circuit Model

Figure 6 is typical of the cross-sections analyzed, and table 6 lists the results of the analysis for all of the cross-sections.

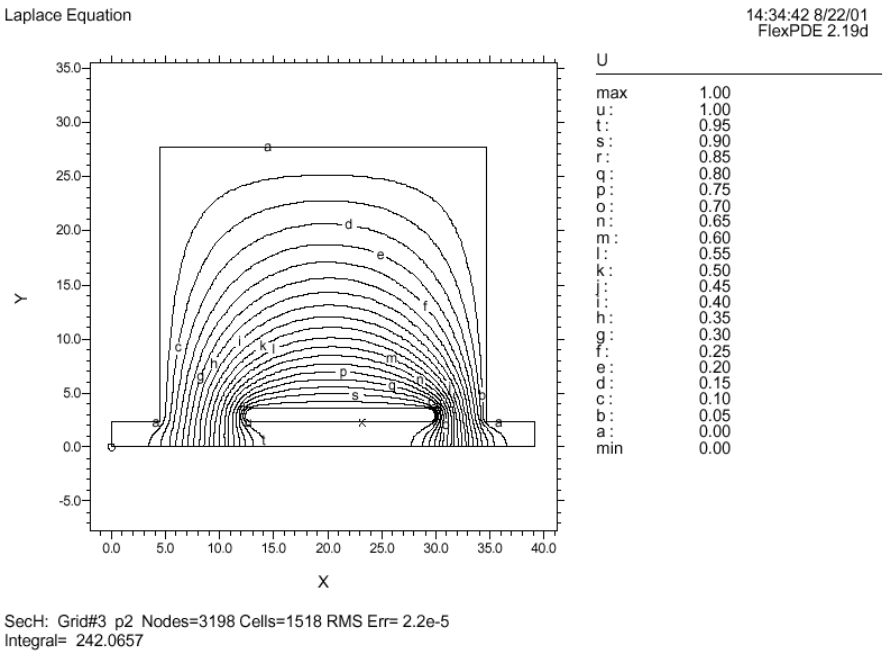

Figure 6: The Equal Potential Plot for Cross-section H

Section	Zo	wl	wd	wo	wi	Ri	Ro
	Ohms	cm	cm	cm	cm	cm	cm
A	64.85	91.19	14.05	12.69	8.38	5.5	6
B	84.16	103.39	21.25	19.72	11.22	10.4	11.7
C	107.25	117.99	27.65	29.08	14.03	19.9	24.4
D	111.03	131.39	36.45	36.75	16.62	28.5	37.2
E	112.48	139.99	41.85	42.07	17.51	37.1	49.3
F	113.56	143.59	44.05	44.59	18.22	46.4	61.5
G	111.88	141.19	42.65	41.89	17.62	54.7	70.7
H	111.76	133.59	36.65	35.95	15.76	62.1	77.3
I	107	123.59	30.05	28.17	13.55	68.3	81.9
J	113.23	111.59	20.45	24.58	11.27	72.8	81.9
K	119.58	104.59	14.65	22.04	9.53	75.7	81.9
L	139.47	96.99	7.25	18.42	6.29	79.1	81.9
M	161.03	94.79	4.25	16.84	4.15	80.6	81.9

Zo: Characteristic Impedance, wl: liner perimeter length, wd: dee perimeter length, wo: liner effective conductor width to equate losses, wi: dee effective conductor width too equate losses, Ri: Distance from inner gap to cyclotron center, Ro: distance from outer gap to cyclotron center.

Table 2: The Results from the Analysis of the Cross-sections

The following table uses the above information and the approximate guided wave length between sections to determine the parameters for an equivalent circuit spanning two cross-sections.

Tline	Length	tau	Zo	wo	wi	C	L
	cm		Ohms	cm	cm	pF	nH
AB	5.7	1.30	74.30	15.95	9.73	0.0072	0.0399
BC	11.3	1.27	95.47	24.10	12.57	0.0096	0.0879
CD	11.4	1.04	109.13	32.77	15.29	0.0002	0.0021
DE	12.4	1.01	111.75	39.35	17.06	0.0000	0.0003
EF	13.6	1.01	113.02	43.32	17.86	0.0000	0.0002
FG	13.1	0.99	112.72	43.23	17.92	0.0000	0.0005
GH	13.2	1.00	111.82	38.84	16.67	0.0000	0.0000
HI	12.5	0.96	109.37	31.90	14.63	0.0003	0.0036
IJ	12	1.06	110.10	26.33	12.38	0.0005	0.0059
JK	7.6	1.06	116.39	23.29	10.38	0.0003	0.0037
KL	8.3	1.17	129.40	20.18	7.80	0.0021	0.0353
LM	3	1.15	150.12	17.62	5.15	0.0006	0.0129

Tline: sections between which the equivalent circuit spans, tau: ratio of impedance between crossections, Zo: effective characteristic impedance, wo effective liner width to preserve losses, wi: effective conductor width to preserve losses, C: additional shunt capacitance needed to preserve stored electric energy, L: additional series inductance need to preserve stored magnetic energy.

Table 3: The Resulting Transmission Line Parameters.

In addition to the lines and circuits specified along the dee, the stem consists of two series connected lines. One of these lines connects from the dee to the liner valley, and the other connects from this point coaxially through the magnet. The cross-section for the line from the dee to the valley floor follows.

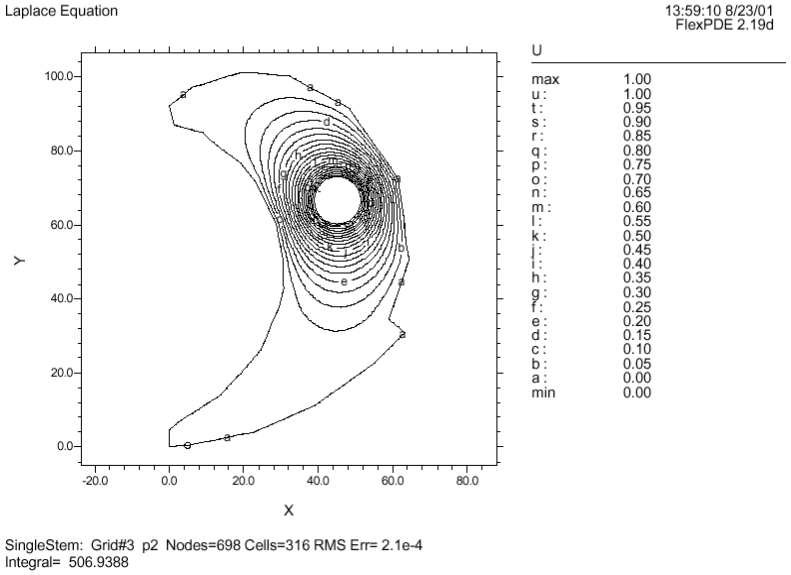

Figure 7: The Tuning Stem spanning Dee to Liner Valley

The stem actually connects to a point referred to as “S” between sections “E” and “F”. The following table list the parameters of the Dee Stem. A resistive annulus serves as the tuning short at the end of the coaxial line S2A.

Tline	Length		Zo	wo	wi
	cm		Ohms	cm	cm
S1A	20.3		72.83	108.00	39.60
S2A	14.6		41.5	39.89	79.8

Table 4: The Tuning Transmission Line Parameters.

The analysis of the cycltron quarter wave (half section) resonator yielded the following results.

Parameter	Circuit Model	Microwave Studio
Injection Voltage	80 KV peak	80 KV peak
Average Extraction Voltage	103.6 KV peak	97.9 KV peak
Frequency	72.4 MHz	72.44 MHz
Tuning Stem Maximum Current	1160 Arms	1416 Arms
Tuning Stem Length (after valley)	14.6 cm	16.4 cm
Tuning Sensitivity (Df/DL)	-0.5 MHz/cm	-0.54 MHz/cm
Power Dissipated per Half Section	6.43 KW	7.35 KW
Unloaded Q	9,524	10,979
Total Power Dissipated (Cyclotron)	51.44 KW	58.8 KW
Stored Energy	0.1414	0.1773
Shunt R (for half section @ 80 KV Peak)	498 Kohms	435.4 Kohms
Shunt C (for half section @ 80 KV Peak)	44.18 pF	55.4 pF
Shunt L (for half section @ 80 KV Peak)	109.4 nH	87.13 nH

Table 5: The Analysis Results.

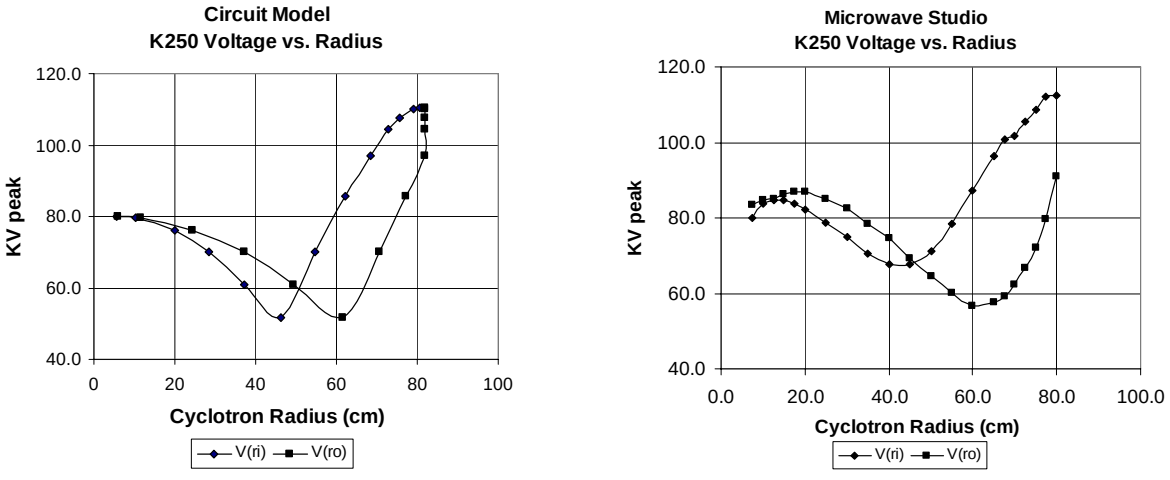

Figure 8: Approximate Dee Voltage versus Cyclotron Radius

Summary and Concluding Statements

Final designs for a K250 medical cyclotron are being developed by ACCEL [1]. This paper has developed a formal method to minimize the conduction losses of rf resonators used as charged particle accelerators. This method was applied to find a near optimum shape for the dees of this cyclotron. The proposed resonator was modeled and analyzed at NSCL using an equivalent circuit technique [3] and then checked with a full 3D modeler [7] by ACCEL. The results presented in table 5 and figure 8 have been manipulated by the author to provide for direct comparison.

Although the results compare favorably, the author postulates that the error may be due to the method of determining the voltage applied against the 3D model. External integration methods applied to the results of finite deference packages are very sensitive to small errors. Some evidence of possible integration problems may be seen on the Microwave Studio Results graph presented in figure 8. This graph shows a voltage difference of ~ 4KV at the center across 2 cm copper perpendicular to the wave direction. This is not a likely result. Since a 5% error in voltage calculation would result in a 10% change in stored energy and conduction losses. A skew of this magnitude would have a significant effect on the element values of the equivalent shunt circuit elements.

References

1) Product Brochure: " Superconducting Cyclotron Contract awarded by Paul Scherrer Institute (PSI), Villigen, Switzerland", "Dr. Detliedf Krischel – ACCEL Instruments GmbH – Friedrich-Ebert-Strabe 1 – D-51429 Bergisch Gladbach"
2) H. G. Blosser, et. al. , "Proposal for a Manufacturing Prototype SUPERCONDUCTING CYCLOTRON for Advanced Cancer Therapy", The National Superconducting Cyclotron Laboratory, Michigan State University, MSUCL-874, 1993
3) J. Vincent, "Modeling and Analysis of RF Structures using an Equivalent Circuit Methodology with Application to Charged Particle Acclerator RF Resonators", UMI # 961355, UMI Company, Ann Arbor, MI, 48103, 1996, Internet. Available from http://www.3pco.com/content/Thesis/Thesis.pdf; accessed April 16, 2001
4) J. Vincent, "INEXPENSIVE RF MODELING AND ANALYSIS TECHNIQUES AS APPLIED TO CYCLOTRONS", Proc. Of the 16th Intl. Conf. On Cyclotrons and their Applications, East Lansing, Michigan, May 2001, to be published by AIP.
5) FLEXPDE software, PDE Solutions Inc., Internet. Available from http://www.flexpde.com/; accessed 16 April, 2001
6) WAC Software, Precision Power Products, Internet. Available from http://www.3pco.com/; accessed 16 April, 2001.
7) CST Microwave Studio software, Computer Simulation Technology Co., Internet. http://www.cst.de; accessed 7 December 2001.